10TH INTERNATIONAL SYMPOSIUM ON PARTICLE IMAGE VELOCIMETRY – PIV13
Delft, The Netherlands, July 1-3, 2013

Tomographic PIV measurement of flow in a complex geometry of nasal cavity

Sunghyuk Im[1], Go Eun Heo[2] , Hyung Jin Sung[1] and Sung Kyun Kim[2]

[1] School of Mechanical Aerospace & Systems Engineering, KAIST, Daejeon, Korea
hjsung@kaist.ac.kr

[2] Department of Mechanical Engineering, Konkuk University, Seoul, Korea

ABSTRACT

Flow inside a scaled model of nasal cavity was measured by tomographic PIV. The model was constructed with transparent silicon. A refractive index of working fluid was matched to the model index by mixing glycerol and water. Four cameras and double pulse laser system were used for tomographic PIV. To obtain high SNR, red fluorescence particles and longpass glass filters were used. A complex model shape was estimated by accumulating three-dimensional particle positions obtained by least square based triangulation. Morphological operations such as opening and closing were used to improve the estimation quality. The geometry information was used to distinguish the fluid and solid regions in the tomographic reconstruction procedure. The model estimation and tomographic reconstruction procedures were evaluated by synthetic image test. The synthetic images were generated by placing a computer model (stereolithography file from CT data) to a virtual 3D coordinates and by seeding particles in the flow region randomly. Perspective transformation matrix for synthetic image generation was adopted from the experimental camera matrix. The synthetic image test shows that the reconstruction quality for a complex 3D geometry was improved by a masking technique. Finally, flow velocity field was calculated from 3D cross-correlation of reconstructed voxel intensities.

1. INTRODUCTION

The nasal cavity in humans is the first point of gas exchange in the respiratory system. As such, the nasal cavity provides a variety of functions and its geometry is very complex. An understanding of the airflow inside the nasal cavity is important to physiological and pathological analyses. Thus, the flow characteristics inside the nasal passage have received significant attention from researchers.

Hopkins et al. (2000) used experimental approaches to develop a methodology for the in vitro measurement of nasal flow using a transparent silicon model and a refractive index-matched working fluid. They used planar particle image velocimetry (PIV) techniques to measure the two-dimensional two-component (2D-2C) velocity field inside a nasal model. Kim and Chung (2004) performed 2D-2C planar PIV measurements and developed a tomographic approach to reconstructing the disordered 3D nasal geometry using a series of 34 sagittal planes. They interpolated the outlines of the shapes in 34 sagittal planes to reveal the coronal plane geometry. Recently, Spence et al. (2011) performed 2D-3C flow measurements using stereoscopic PIV, and a series of the traversed 2D-3C maps was used to reconstruct the 3D-3C volumes. These studies relied on the 2D cross-sectional images acquired in the sagittal plane to obtain a 3D geometric reconstruction and the flow pattern measurements.

In the present study, transparent phantom model of nasal cavity was constructed using rapid prototype (RP) techniques. The refractive index of the working fluid was matched to the index of silicon by mixing water and glycerol. The camera was calibrated by placing a calibration target in an acrylic box of the same size filled with the refractive index-matched working fluid. A volume self-calibration was performed to compensate for any calibration errors. The experimental images were pre-processed by subtracting the temporal averaged image to reduce the background noise. The 3D coordinates of each fluid tracer particle were calculated by iterative least-squares triangulation and were accumulated in the sub-volume space for model estimation. The morphological operations and upsampling steps were successively applied to the accumulation data to increase the model estimation accuracy. The obtained nasal geometry was used as a mask to increase the quality of the tomographic voxel reconstruction. Finally, the flow velocity inside the obtained nasal geometry was measured by cross-correlation analysis. The analysis procedures, model estimation, and tomographic reconstruction steps were qualified using a synthetic image test. The test showed the validity of the model estimation and tomographic reconstruction algorithms.

2. EXPERIMENTAL METHOD

First, the nasal geometry data were captured using medical CT imaging techniques. A negative nasal model was constructed with water-soluble material using rapid prototype (RP) machines. The negative model was placed in an acrylic box to construct a transparent flow phantom model. Transparent silicon was poured into the

box and cured at room temperature over 2 days. Flow phantom model was constructed by removing the negative model. Refractive index-matching between the working fluid and the model itself was crucial for preventing optical distortions of the light. Water and glycerol were used to match the refractive index of the working fluid to the silicon model. The mixing ratio was fine-tuned by measuring the distortion of the background grid lines.

The nasal passage was connected to a flow circulating system configured with a reservoir, valves, a pump, and a flow meter. The working fluid comprising a mixture of water and glycerol was driven by a hydraulic pump to produce a steady flow through the circulating system. The flow rate of the working fluid was monitored and controlled using a turbine flow meter and the valves, and the working fluid was stored in a reservoir.

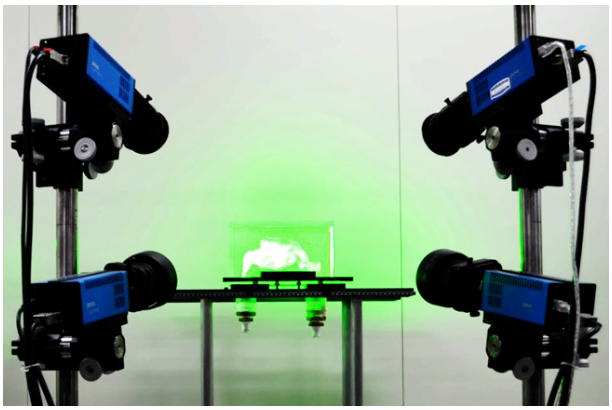

Figure 1 Experimental configuration of flow phantom model and cameras

The test volume was illuminated by a Nd:YAG double pulse laser emitting a 532 nm beam at 15 Hz. The laser beam was expanded to illuminate the whole test volume using a combination of optical lenses. The 3D flow field was characterized using the tomographic PIV technique by acquiring images using four high-speed cameras (Fig. 1). The cameras were used in a successive double shutter mode. Each camera was synchronized with the laser using a pulse/delay generator. An 85 mm tilt-shift lens with f/8, which satisfied the Scheimpflug principle, was attached to each camera. Red fluorescence particles and long-pass glass filters were used to increase the signal-to-noise ratio in the PIV images. The captured images were passed through a temporal filtering algorithm to remove the background noise by subtracting the temporally averaged images.

The camera images were calibrated by obtaining a mapping function, the perspective transformation matrix $\mathbf{P}_c$. The mapping function satisfies the 3D to 2D transform relation $\mathbf{x}_c=\mathbf{P}_c\mathbf{X}$ where $\mathbf{x}_c$ and $\mathbf{X}$ are the 2D and 3D coordinates, respectively. The real (3D) and image (2D) coordinates of the control points were obtained using a calibration object in a V-shape. A calibration object was placed in the acrylic box filled with a refractive index-matched working fluid to model the encasing of the experimental target (i.e., the transparent silicon model) encased in an acrylic box (Fig. 2). Although the optical configuration used during the camera calibration steps was the same as the configuration used during the experimental measurements, a certain degree of measurement noise was inevitable due to the perturbation of model position and refractive index mismatching. A volume self-calibration step was applied to compensate for these errors.

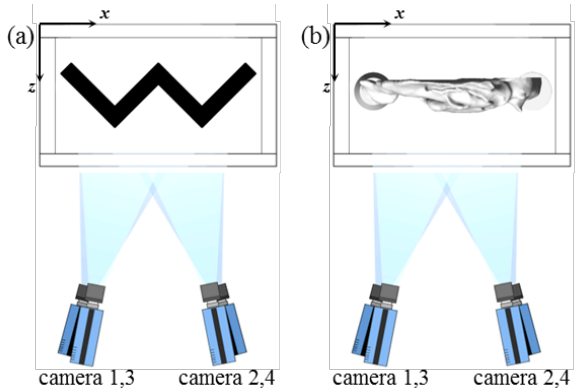

Figure 2 (a) Camera calibration configuration and (b) configuration for flow measurement

3. ANALYZING ALGORITHMS

3.1. Geometry acquisition and PIV calculations

In most flow measurement experiments, the full field of view is filled by a fluid region. Knowledge of the shape of a fluid region is important because it helps us understand and analyze the flow patterns in a complex nasal geometry. As a first step toward acquiring the three-dimensional geometry of the nasal cavity, 2D point coordinates $\mathbf{x}_c$ were detected with sub-pixel accuracy in each camera *c*. The 2D particles identified in each camera image were paired to obtain the 3D coordinates $\mathbf{X}$. The 3D coordinates of a particle $\mathbf{X}$ were then obtained by triangulation (Hartley, 1997). The particle pairing procedure used during the volume self-calibration steps, shown in Fig. 3, was adapted to identify all possible particle pairs. If a set of candidate particles satisfied the pairing criteria, the triangulated coordinates $\mathbf{X}_p$ were converted to the indices of the sub-volumes comprising a bundle of voxels 8×8×8 [vx^3]. An accumulated particle number variable *SV* was initialized to zero and incremented according to the indices. The geometry shape can be constructed with fewer images when the particles were accumulated into the sub-volumes. It was therefore not necessary to accumulate particles within each voxel.

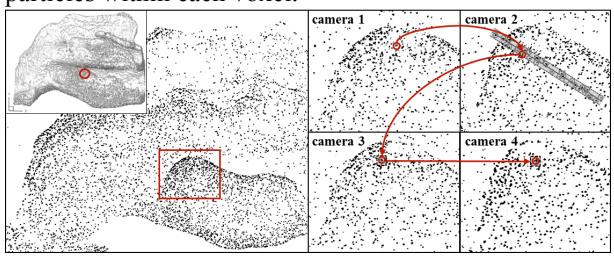

Figure 3 Particle triangulation procedure

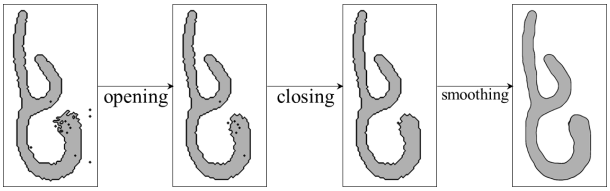

Figure 4 Cross-sectional images of the morphological operation results

False positioning errors occurred during the triangulation process due to mispairing between the particle candidates in each camera image. The large number of particles present in each image increased the number of possible pairing options in the matching process. Many mispairing errors could be neglected by applying a threshold to the accumulated value and morphological operations. The morphological operations consist of opening and closing using binary erosion and dilation. As shown in Fig. 4, a clear shape of the model could be obtained using the morphological operations. The estimated model data $SV(i,j,k)$ was upsampled to voxel wise data $M(x,y,z)$ using Gaussian interpolation. The upsampled geometry data were regarded as a mask variable $M(x,y,z)$ and provided the criterion for distinguishing the fluid from the solid regions. The multiplicative line of sight (MLOS) estimation and simultaneous multiplicative algebraic reconstruction technique (SMART) iterations, i.e., the MLOS-SMART algorithm, was implemented and modified using $M(x,y,z)$ to avoid unnecessary computations. Finally, the flow velocity field was calculated based on a direct non-zero voxel cross-correlation analysis.

3.2. Synthetic image test

Synthetic image tests are widely used to validate PIV algorithms. The mapping function determined during the experimental camera calibration steps was adapted to the camera configuration of the synthetic image test. The shapes of the original 3D model were imported from the STL file to construct a mask $M(x,y,z)$. The 3D surface data was introduced into virtual 3D space and converted into volume data. The mask voxels inside the nasal cavity were then set to one, and the outside voxels remained zero. Several particles were randomly generated and distributed across the voxels that had been assigned a mask value of one. The 3D particle coordinates $\mathbf{X}_p$ for each particle p were projected onto each 2D image plane by applying the perspective transformation $\mathbf{x}_{p,c}=\mathbf{P}_c\mathbf{X}_p$ for each camera c. The total number of particles was determined according to the PPV value multiplied by the number of non-zero voxels of the mask.

The procedure described in Section 3.1 was tested by applying the procedure to the generated images. A series of 1000 synthetic images was generated to permit position accumulation. The initial 3D geometry estimate was obtained by accumulating triangulated particles from the series of generated images. The quality of the model estimation increased as a result of the morphological operations and Gaussian upsampling techniques. The acquired mask shows 95.74% of similarity to the original geometry.

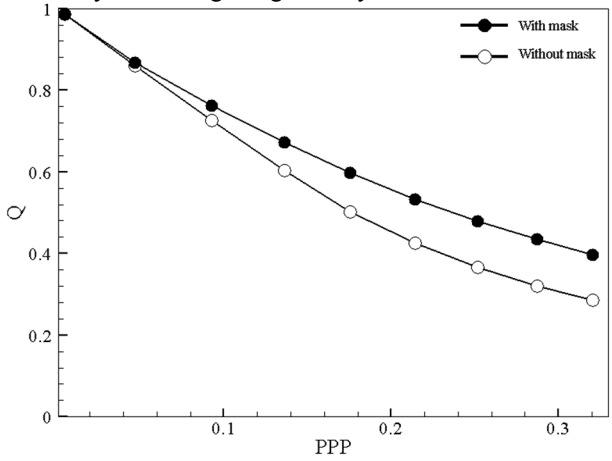

Figure 5 Cross-sectional images of the morphological operation results

The acquired mask was applied to the tomographic reconstruction algorithm. The higher-quality voxel reconstruction algorithm could be used to obtain the acquired geometry information. Figure 5 shows the quantitative reconstruction quality measurement results. At low particle densities, the reconstruction quality approached a value of one, indicating that the intensity distributions were identical. The quality decreased as the particle density increased. A quality improvement of about 10% was obtained using the three-dimensional geometry mask in the tomographic reconstruction

4. RESULTS AND DISCUSSION

The geometry of a transparent nasal model was acquired by accumulating the triangulated 3D particle positions and applying morphological operations and Gaussian upsampling procedures. A series of 3D-3C instantaneous flow fields was measured and time-averaged using the aforementioned methods. The Reynolds number associated with the inspiration flow at the nasal inlet was Re=400, where the characteristic length is the hydraulic diameter at the nostril of the model.

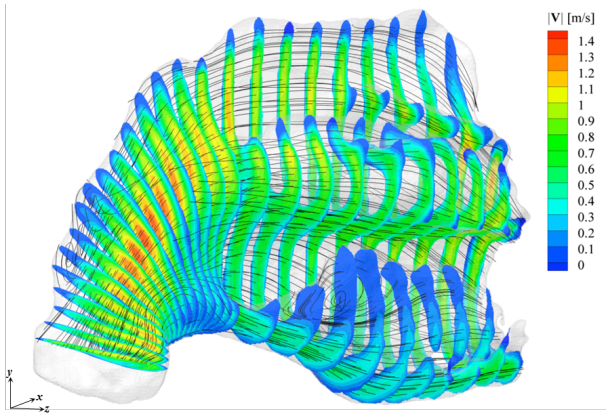

Figure 6 Measured velocity field and streamlines

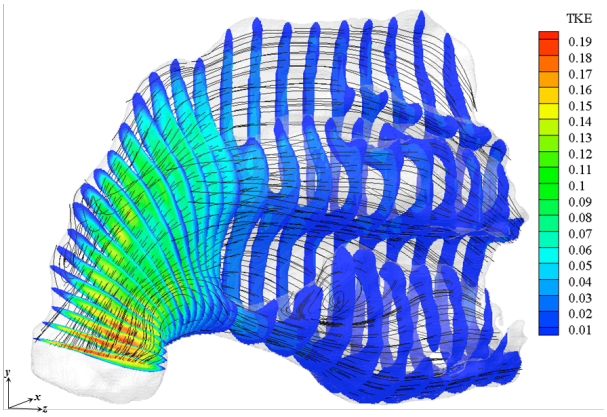

Figure 7 Calculated turbulence kinetic energy and streamlines

Figure 6 and Fig. 7 show contour maps and the streamlines in the coronal cross-sectional planes, where the contours indicate the magnitude of the velocity |V| and the turbulence kinetic energy (k), respectively. Coronal cross-sectional images were extracted along the plane normal to the direction of the main flow stream. The velocity magnitude contours shown in Fig. 18a revealed the flow distribution over the nasal cavity. In the region from the nostril to the front of the meatuses, the main stream tended to pass through the upper region. Very low velocities were observed in the inferior nasal meatus, whereas the velocity magnitude in the nasal passage was relatively high, except in the inferior meatus. The value of k decreased over the curved expander and settled at a low value, indicating a low k generation. The vector fields, streamlines, and turbulence kinetic energy were obtained and analyzed to identify the flow characteristics inside the nasal model. We hope that the present method will be helpful for measuring flow fields inside a complex geometry, and the measured flow data will be useful for analyzing medical images of nasal cavities.

ACKNOWLEDGMENTS

This study was supported by the Creative Research Initiatives (No. 2013-003364) program, and partially supported by the World Class University (R31-2008-000-10045-0) program and the Basic Science Research program (No. 2011-028942) of the National Research Foundation of Korea.

REFERENCES

[1] Hopkins, L., J. Kelly, et al. "Particle image velocimetry measurements in complex geometries." Experiments in Fluids 29-1 (2000) pp.91-95

[2] Kim, S. K. and S. K. Chung "An investigation on airflow in disordered nasal cavity and its corrected models by tomographic PIV." Measurement Science and Technology 15-6 (2004) pp.1090-1096

[3] Spence, C. J. T., N. A. Buchmann, et al. "Stereoscopic PIV measurements of flow in the nasal cavity with high flow therapy." Experiments in Fluids 50-4 (2010) pp.1005-1017

[4] Wieneke, B. "Volume self-calibration for 3D particle image velocimetry." Experiments in Fluids 45-4 (2008) pp.549-556

[5] Sonka et al. "Image Processing, Analysis and Machine Vision" PWS publishing, Boston (1999)

[6] Elsinga, G., F. Scarano, et al. "Tomographic particle image velocimetry." Experiments in Fluids 41-6 (2006) pp.933-947

[7] Atkinson, C. and J. Soria "An efficient simultaneous reconstruction technique for tomographic particle image velocimetry." Experiments in Fluids 47-4 (2009) pp.553-568